IMMUNOHISTOCHEMICAL LOCALIZATION OF HISTIDINE-RICH GLYCOPROTEIN IN HUMAN SKELETAL MUSCLE: PREFERENTIAL DISTRIBUTION OF THE PROTEIN AT THE SARCOMERIC I-BAND

L. Mattii[1], L. Rossi[1], C. Ippolito[1], G. Alì[2], D. Martini[3], A. Raggi[3], A.R.M. Sabbatini[3]

[1]Dipartimento di Medicina Clinica e Sperimentale, Università di Pisa, Pisa, Italy;
[2]U.O. Anatomia Patologica III, Azienda Ospedaliero-Universitaria Pisana (AOUP), Pisa, Italy.
[3]Dipartimento di Patologia Chirurgica, Medica, Molecolare e dell'Area Critica, Università di Pisa, Pisa, Italy;

Corresponding author: Antonietta R.M. Sabbatini, M.D., Dipartimento di Patologia Chirurgica, Medica, Molecolare e dell'Area Critica, Università di Pisa, via Roma 55, 56126 Pisa, Italy.
Phone: +39.050.2218-681, Fax: +39.050.2218-660, E-mail: antonietta.sabbatini@med.unipi.it

ABSTRACT

Histidine-rich glycoprotein (HRG) is a relatively abundant plasma protein that is synthesized by parenchymal liver cells. Using Western blot analysis and immunoperoxidase techniques, we have previously shown the presence of HRG in human skeletal muscle. This paper reports the results of immunofluorescence experiments carried out on sections of human normal skeletal muscle biopsies to investigate the subcellular localization of HRG. The HRG localization was also compared with that of skeletal muscle AMP deaminase (AMPD1) since we have previously described an association of the enzyme with the protein. The obtained results give evidence for a preferential localization of HRG at the I-band level, where it shows the same distribution of actin and where AMPD1 is present in major concentration.

Keywords: Histidine-rich glycoprotein, skeletal muscle, AMP deaminase, metallochaperone, immunofluorescence.

Abbreviations: (HRG) Histidine-rich glycoprotein, (AMPD1) skeletal muscle AMP deaminase, (TnT) troponin T, (FGF-2) fibroblast growth factor-2, (HUVEC) human umbilical vein endothelial cells.

INTRODUCTION

Histidine-rich glycoprotein (HRG), also known as histidine-proline-rich glycoprotein, is a 75 kDa glycoprotein originally isolated and characterized from human serum (Haupt and Heimburger 1972; Heimburger et al. 1972) and later found in the plasma of many other vertebrates where it is present at relatively high concentrations (100-150 μg/ml in humans) (Morgan et al. 1978). It is synthesized by parenchymal liver cells (Koide et al. 1986) and although it has also been detected in immune cells such as monocytes and macrophages (Sia et al. 1982) as well as in the α-granules of platelets and in megakaryocytes (Leung et el. 1983), a study on the cellular origin of murine plasma HRG has shown that HRG mRNA is produced exclusively in the liver (Hulett and Parish 2000). HRG interacts with many ligands including fibrinogen, plasminogen, plasmin, heparin and heparin sulphate, IgG, FcgR, C1q, tropomyosin, thrombospondin and divalent transition metal cations such as Zn^{2+}. Through its multidomain structure, HRG might act as an adaptor protein that brings together different ligands under specific conditions, modulating many physiological processes such as coagulation, fibrinolysis, cell chemotaxis, immune response, apoptotic process, cell adhesion and migration, cell growth and proliferation (Jones et al. 2005). The association of HRG with purified rabbit skeletal muscle AMP deaminase (AMPD1) has been previously described by our research group (Ranieri-Raggi et al. 1997, 2003). AMPD1, one of the three enzymes of the purine nucleotide cycle, catalyzes the deamination of AMP to IMP playing a central role in preserving the adenylate energy charge in myocytes following exercise (Lowenstein and Tornheim, 1971). It has also given experimental evidence that rabbit HRG hosts two Zn^{2+} ions coordinated by His residues and sulfur from cysteine residues strengthening the hypothesis that HRG functions as a metallochaperone in the formation of a heterodimer with skeletal muscle AMPD (Mangani et al. 2003; Ranieri-Raggi et al. 2014; Ronca and Raggi, 2015).

We have provided the first evidence for the presence of HRG in human skeletal muscle showing that an antibody against human plasma HRG binds to muscle fibers (Sabbatini et al. 1999). Moreover, in a study on the origin of skeletal muscle HRG, we have demonstrated that muscle cells do not synthesize the protein but instead can actively internalize it from plasma, indicating for the first time that HRG can be carried to tissues via circulation (Sabbatini et al. 2011). We have also described a positive correlation in human skeletal muscle between the content of HRG and the level of AMPD1 activity that it is known to be predominant in type IIB fast-twitch glycolytic fibers (Sabbatini et al. 1999, 2006).

This paper reports the results of an immunohistochemical study carried out to investigate the subcellular localization of HRG in human skeletal muscle. In particular, the HRG distribution at the sarcomeric level was evaluated and also compared to that of AMPD1.

MATERIALS AND METHODS

Antibodies and reagents

Rabbit anti-HRG polyclonal antibody (HRG-462) raised against the C-terminal region (residues 462-471) of human plasma HRG and rabbit anti-human AMPD1 polyclonal antibody were produced in-house as previously described (Sabbatini et al. 1999, 2006). Rabbit anti-HRG polyclonal antibody (HRG-256) against the 256-270 region of human plasma HRG, mouse anti-skeletal myosin (fast) clone My-32 , that stains the type II (fast-twich) fibers, and mouse anti-actin (α-sarcomeric) monoclonal antibodies were purchased from Sigma-Aldrich (Saint Louis, Missouri, USA). Alexa Fluor® 488 goat anti-rabbit IgG (H+L) and Alexa Fluor 568 donkey anti-mouse IgG secondary antibodies (for optical immunofluorescence microscopy), Alexa Fluor 488 goat anti mouse IgG and Alexa Fluor® 568 donkey anti-rabbit IgG secondary antibodies (for confocal microscopy) were purchased from Invitrogen (Carlsbad, California, USA). Nuclear dye TO-PRO (TO-PRO®-3stain) was from Life Technologies Italia (Monza, MB, Italy). All other reagents were of analytical grade and were purchased from Sigma-Aldrich and Fluka (Buchs, Switzerland).

Sample collection

Three muscle biopsies, one from gastrocnemius (male, patient age = 28), and two from quadriceps femoris (females, patient age = 69 and 78), were selected among frozen muscle samples from the archives of Division of Pathology, Department of Surgical, Medical, Molecular Pathology and Critical Care, University of Pisa. Serial sections of 8 μm were cut in a cryostat at -20 °C and processed for routine histological and histochemical stains, i.e. hematoxylin-eosin, succinate dehydrogenase, NADH tetrazolium reductase, routine ATPase (pH 9.4), ATPase pre-incubated at pH 4.3 and 4.6 (Dubowitz and Brooke, 1973) and for immunofluorescence microscopy. All the procedures performed in the present study involving human participants were in accordance with the 1964 Helsinky Declaration and its later amendments.

Immunofluorescence Microscopy

Tissue sections were fixed in cold acetone/methanol (1:1 v/v) for 10 min at -20 °C, washed in phosphate buffered saline (PBS) and incubated with 0.2% Triton-X100 in PBS for 10 min. After one hour in blocking solution (0.1% Tween, 0.25% BSA in PBS) slides were incubated for 16 hours

at 4 °C with primary antibodies diluted in blocking solution as follows: anti-human HRG polyclonal antibodies (1:500), anti-myosin My-32 monoclonal antibody (1:750), anti-actin (α-sarcomeric) monoclonal antibody (1:300), anti AMPD1 polyclonal antibody (1:400). Slides were then washed three times with blocking solution and incubated for 1.5 hours in the dark with relative fluorescent secondary antibodies diluted 1:250 in blocking solution. For confocal microscopy, nuclear staining was performed by TO-Pro. Samples were mounted with PBS-glycerol solution. All steps were performed at room temperature unless otherwise specified. Negative controls for secondary antibodies were performed omitting primary antibodies and incubating the specimens with nonimmune serum. The specificity of the produced in-house primary antibodies was previously tested by Western blot analysis (Sabbatini et al. 1999, 2006) and, in the present study, by anti-HRG and anti-AMPD1 immunoglobulins pre-adsorbed for 16 hours at 4 °C with a ten fold excess of the respective blocking peptides, i.e. the synthetic peptide used for rabbit immunization. The analysis of immunofluorescence pattern was performed in at least three non-consecutive sections for each sample. Specimens were observed by a Zeiss Axioplan microscope, equipped with a Nikon digital camera, using x40 or x100 oil immersion lenses or by confocal laser scanning microscopy (TC SSP8 Leica Microsystems, Mannheim, Germany) using a x63 oil immersion lens and 488 nm, 561 nm and 642 nm excitation wavelength lasers. Confocal multiple optical sections (Z planes = 23, z-step = 0.35μm) were used to obtain the maximum intensity projections and the isosurface representation showed in the present paper.

RESULTS AND DISCUSSION

We have provided the first evidence for the presence of HRG in human skeletal muscle (Sabbatini et al. 1999). Moreover, we have shown that muscle cells do not synthesize the protein but instead can actively internalize it from plasma, demonstrating for the first time that HRG can be carried to tissues via the circulation (Sabbatini et al. 2011). Our results have been confirmed by recent *in vivo* experiments with radiolabeled HRG showing that, after intravenous injection, HRG was internalized quickly in healthy tissues, including muscle, and in tumors (Tugues et al. 2014).

At present no information is reported in literature about the subcellular localization of HRG in muscle fibers. To address this issue we carried out the present immunohistochemical study on three biopsies of human skeletal muscle.

The muscle fibers of the three specimens, that showed no histological or histochemical abnormalities, appeared highly contracted. Comparable immunohistochemical results were obtained for all the tested antigens using each of the three biopsies. The immunohistochemical analysis for HRG was performed using both the HRG-462 and the commercial HRG-256 antibodies that

showed the same pattern of positive staining in all the samples analyzed. Fig. 1a shows as an example the staining obtained in optical fluorescence microscopy using the two anti-HRG antibodies. Neither autofluorescent nor immunofluorescent signals could be observed in negative controls with 488 nm, 561 nm and 642 nm excitation lasers.

By optical fluorescence microscopy all the cross sections exhibited a diffuse, uniform immunoreactivity for HRG in the connective tissue among the muscle fibers. Conversely, within the fibers a speckled staining pattern characterized by dots, lines or star-shaped structures was observed (Fig. 1a). According to the intensity of sarcoplasmic fluorescence, two fiber-types could be distinguished, one weakly stained and another with a stronger signal due to more abundant, larger and brighter granulations. Double immunofluorescence with anti-HRG and anti-myosin My-32 antibodies evidenced, in cross sections, a granular pattern for HRG that filled the sarcoplasmic spaces free from myosin (Fig. 1b). Moreover, the highest HRG positivity was observed in type II fibers, in agreement with our previous observations (Sabbatini et al. 1999). The same double immunoreaction, performed on longitudinal sections (Fig. 1c), showed a cross-striation pattern for HRG at the myofibrillar level. The HRG signal was alternated to that of myosin suggesting an association of HRG to the I-band although an overlapping of the two signals at the border between the I-band and the A-band cannot be excluded.

The sarcomeric localization of HRG observed with the light microscope was further characterized by confocal laser scanning microscopy (Fig. 2). The sarcomeric structure was identified evidencing the I-band by the anti-actin antibody whilst the periphery of the A-band was evidenced by the anti-myosin My-32 antibody (Fig. 2a). The double staining carried out with the anti-HRG antibody and the anti-myosin or the anti-actin antibody confirmed the localization of HRG at the level of the I-band. In particular, the longitudinal sections showed a specific, periodic distribution of HRG over the muscle fiber that consisted of sharp, fluorescent bands. The bands were as wide as the whole I-band of the sarcomere, making contact with the ends of the A-band (Fig. 2a, b). Both in longitudinal and in cross sections, HRG showed the same sarcomeric localization of actin although the two proteins did not co-label as evidenced in merged images (Fig. 2a-d).

Our investigation was also addressed to compare the subcellular localization of HRG and AMPD1 as we have previously described the association of HRG with purified rabbit AMPD1 (Ranieri-Raggi et al. 1997, 2003) and showed that an anti-HRG antibody bound mainly to type IIB fibers of human skeletal muscle that are well known to contain the highest level of AMPD1 activity (Sabbatini et al. 1999). All the longitudinal sections analyzed by confocal microscopy showed a periodical distribution of AMPD1 over the muscle fibers. Specifically, at sarcomeric level the

AMPD1 staining was very strong all over the I-band, similarly to the distribution of HRG, although a positive staining could also be clearly detected into the A-band (Fig. 3).

The observation that AMPD1 is detectable into the A-band is in agreement with Ashby et al. (1979) and van Kuppevelt et al. (1994) that describe the enzyme, in unstretched/contracted muscle, predominantly over the I-band and to a minor extent in the middle of the A-band and, in stretched muscles, at the boundary of A- and I-band. It should be noted that AMPD1 has been found to bind native myosin and purified myosin S2 fragments (Ashby and Frieden 1977, Ashby et al. 1979). It has also been suggested that AMPD1 may be attached to the myofibrils through titin molecules and this immobilization could improve its metabolic efficiency (Cooper and Trinick 1984). However, no clear influence on AMPD1 activity has been found as a result of the interaction of the enzyme with either titin or myosin. In contrast, an involvement of the N-terminal Zn-binding region of troponin T (TnT) in the modulation of AMPD1 activity has been observed *in vitro* (Ranieri-Raggi et al. 1985) that let us to suppose that an interaction between the N-terminal Zn-binding regions of AMPD1 and TnT could also occur *in vivo* (Ronca and Raggi 2017). In the light of the results of this paper, the different sarcomeric distribution of HRG and AMPD1 together with their co-localization at the I-band suggests that HRG might move from extracellular space to sarcoplasm and myofibrils through Tranverse tubuls, accumulating primarily at the triad level where it can supply zinc to AMPD1, by acting as zinc chaperone.

The main result of the present study remains the observation of a preferential localization of HRG at the sarcomeric I-band. This finding deserves consideration as it suggests that HRG could interact with proteins that take part to the constitution of the thin filament. The data of the literature mentioned below support this hypothesis. First, an interaction between HRG and sarcomeric tropomyosin could take place in the light of the observation that HRG binds with high affinity and in a Zn^{2+} or pH dependent manner to tropomyosin present on the surface of the FGF-2-activated HUVEC cell (Guan et al. 2004). Secondly, an interaction between HRG and a component of the troponin complex, namely TnT, could also be hypothesized. The N-terminal region of fast skeletal TnT contains a putative zinc-binding site (Ronca and Raggi 2017). Interestingly, it has been reported that the AMPD1 allosteric properties, removed by limited proteolysis of the N-terminal region of the enzyme, can be restored by TnT or the phosphorylated N-terminal region of TnT (Ranieri-Raggi et al. 1985). HRG is a regulatory component of AMPD1 and, behaving as zinc metallochaperone, may enhance the *in vivo* AMPD1 stability through insertion of zinc, essential for its activity, or modulating its intracellular availability (Mangani et al. 2003, 2007; Martini et al. 2007). Therefore it could be hypothesized that the unrestrained AMPD1 activity that follows the N-

terminus proteolytic cleavage of the enzyme in strenuously exercised muscle could be counteracted by the binding of HRG-AMPD1 to TnT (Ronca and Raggi 2017).

The present paper also shows a nuclear localization of HRG (Fig 2e). This observation deserves consideration since HRG regulates numerous biological activities including cell adhesion and cell proliferation. In particular, a relationship between HRG and rearrangement of actin cytoskeleton has been described. On human lymphocytes and leukemic T-cell line, HRG promotes morphological changes that are associated not only with the formation of pseudopodia-like structures but also with an increase in the F-actin rich surface protrusion (Ohta et al. 2009). Furthermore, it has been described that HRG, by inducing focal adhesion kinase phosphorylation, targets focal adhesions in endothelial cells disrupting the actin stress fibers formation and therefore exhibiting an antiangiogenic activity (Lee et al. 2006).

Further studies will be necessary to deepen the ultrastructural localization of HRG in muscle fiber, both at sarcomeric and nuclear level, as well as to better clarify its possible role in relation to gene transcription and regulation.

Acknowledgements: We thank Dr Enza Polizzi and Sauro Dini for skilled technical assistance.

Funding Informations: This research was supported by a grant from the University of Pisa.

Conflict of interest: The authors who have taken part in this study declare that they have no conflicts of interest in the research.

Ethical approval: All the procedures performed in the present study involving human participants were in accordance with the 1964 Helsinky Declaration and its later amendments. For this type of study, conducted retrospectively, formal consent was not required.

REFERENCES

Ashby B, Frieden C (1977) Interaction of AMP-aminohydrolase with myosin and its sufragments. J Biol Chem 252:1869-1872

Ashby B, Frieden C, Bischoff R (1979) Immunofluorescent and histochemical localization of AMP deaminase in skeletal muscle. J Cell Biol 81:361-373

Cooper J, Trinick J (1984) Binding and location of AMP deaminase in rabbit psoas muscle myofibrils. J Mol Biol 177:137-152

Dubowitz V, Brooke MH (1973) Muscle Biopsy: A modern Approach. WB Saunders, London, Philadelphia, Toronto

Guan X, Juarez JC, Qi X, Shipulina NV, Shaw DE, Morgan WT, McCrae KR, Mazar AP, Doñate F (2004) Histidine-proline-rich glycoprotein (HRG) binds and transduces anti-angiogenic signals through cell surface tropomyosin on endothelial cells. Thromb Haemost 92:403-412

Haupt H, Heimburger N (1972) Human serum proteins with high affinity for carboxymethylcellulose. I. Isolation of lysozyme, C1q and 2 hitherto unknown globulins. Hoppe Seylers Z Physiol Chem 353: 1125-1132

Heimburger N, Haupt H, Kranz T, Baudner S (1972) Human serum proteins with high affinity to carboxymethylcellulose. II. Physico-chemical and immunological characterization of a histidine-rich 3,8S-2-glycoprotein (CM–protein I) Hoppe Seylers Z Physiol Chem 353: 1133-1140

Hulett MD, Parish CR (2000) Murine histidine-rich glycoprotein: cloning, characterization and cellular origin. Immunol Cell Biol 78:280-287

Jones AL, Hulett MD, Parish CR (2005) Histidine-rich glycoprotein: A novel adaptor protein in plasma that modulates the immune, vascular and coagulation systems. Immunol Cell Biol 83:106-118

Koide T, Foster D, Yoshitake S, Davie EW (1986) Amino acid sequence of human histidine-rich glycoprotein derived from the nucleotide sequence of its cDNA. Biochemistry 25: 2220-2225

Lee C, Dixelius J, Thulin A, Kawamura H, Claesson-Welsh L, Olsson AK (2006) Signal transduction in endothelial cells by the angiogenesis inhibitor histidine-rich glycoprotein targets focal adhesions. Exp Cell Res 312:2547-2556

Leung LL, Harpel PC, Nachman RL, Rabellino EM (1983) Histidine-rich glycoprotein is present in human platelets and is released following thrombin stimulation. Blood 62:1016-1021

Lowenstein J, Tornheim K, (1971) Ammonia production in muscle: the purine nucleotide cycle. Science 171:397-400

Mangani S, Benvenuti M, Moir AJG, Ranieri-Raggi M, Martini D, Sabbatini AR, Raggi A (2007) Characterization of the metallocenter of rabbit skeletal muscle AMP deaminase. Evidence for a dinuclear zinc site. Biochim Biophys Acta 1774:312-322

Mangani S, Meyer-Klaucke W, Moir AJG, Ranieri-Raggi M, Martini D, Raggi A (2003) Characterization of the Zn binding site of the histidine-proline-rich glycoprotein associated with rabbit skeletal muscle AMP deaminase. J Biol Chem 278:3176-3184

Martini D, Ranieri-Raggi M, Sabbatini ARM, Moir AJG, Polizzi E, Mangani S, Raggi A (2007) Characterization of the metallocenter of rabbit skeletal muscle AMP deaminase. A new model for substrate interactions at a dinuclear cocatalytic Zn site. Biochim Biophys Acta 1774:1508-1518

Morgan WT, Koskelo P, Koenig H, Conway TP (1978) Human histidine-rich glycoprotein. II. Serum levels in adult, pregnant women and neonates. Proc Soc Exp Biol Med 158:647-651

Ohta T, Ikemoto Y, Saeki K, Koide T, Wakabayashi S (2009) Histidine-rich glycoprotein and concanavalin A synergistically stimulate the phosphatidylinositol 3-kinase-independent signaling pathway in leukocytes leading to increased cell adhesion and changes in cell morphology. Cell Immunol 259:5-12

Ranieri-Raggi M, Martini D, Sabbatini AR, Moir AJ, Raggi A (2003) Isolation by zinc-affinity chromatography of the histidine-proline-rich-glycoprotein molecule associated with rabbit skeletal muscle AMP deaminase. Evidence that the formation of a protein-protein complex between the catalytic subunit and the novel component is critical for the stability of the enzyme. Biochim Biophys Acta 1645:81-88

Ranieri-Raggi M, Moir AJ, Raggi A (1985) Interaction with troponin T from white skeletal muscle restores in white skeletal muscle AMP deaminase those allosteric properties removed by limited proteolysis. Biochim Biophys Acta 827:93-100

Ranieri-Raggi M, Moir AJG, Raggi A (2014) The role of histidine-proline-rich glycoprotein as zinc chaperone for skeletal muscle AMP deaminase. Biomolecules 4:474–497

Ranieri-Raggi M, Montali U, Ronca F, Sabbatini A, Brown PE, Moir AJG, Raggi A (1997) Association of purified skeletal-muscle AMP deaminase with a histidine-proline-rich glycoprotein-like molecule. Biochem J 326:641-648

Ronca F, Raggi A (2015) Structure-function relationships in mammalian histidine-proline-rich glycoprotein. Biochimie 118:207-220

Ronca F, Raggi A (2017) Role of troponin T and AMP deaminase in the modulation of skeletal muscle contraction. Rend Fis Acc Lincei 28(1):143-158

Sabbatini ARM, Mattii L, Battolla B, Polizzi E, Martini D, Ranieri-Raggi M, Moir AJ, Raggi A (2011) Evidence that muscle cells do not express the histidine-rich glycoprotein associated with AMP deaminase but can internalise the plasma protein. Eur J Histochem 55:33-38

Sabbatini ARM, Ranieri-Raggi M, Pollina L, Viacava P, Ashby JR, Moir AJG, Raggi A (1999) Presence in human skeletal muscle of an AMP deaminase-associated protein that reacts with an antibody to human plasma histidine-proline-rich glycoprotein. J Histochem Cytochem 47:255-260

Sabbatini ARM, Toscano A, Aguennouz M, Martini D, Polizzi E, Ranieri-Raggi M, Moir AJG, Migliorato A, Musumeci O, Vita G, Raggi A (2006) Immunohistochemical analysis of human skeletal muscle AMP deaminase deficiency. Evidence of a correlation between the muscle HRG content and the level of residual AMP deaminase activity. J Muscle Res Cell Motil 27:83-92

Sia DY, Rylatt DB, Parish CR (1982) Anti-self receptors V. Properties of a mouse serum factor that blocks autorosetting receptors on lymphocytes. Immunology 45:207-216

Tugues S, Roche F, Noguer O, Orlova A, Bhoi S, Padhan N, Akerud P, Honjo S, Selvaraju RK, Mazzone M, Tolmachev V, Claesson-Welsh L (2014) Histidine-rich glycoprotein uptake and turnover is mediated by mononuclear phagocytes. PLoS One 9:e107483 Erratum in: PloS One (2015) 10:e0118636

van Kuppevelt TH, Veerkamp JH, Fishbein WN, Ogasawara N, Sabina RL (1994) Immunolocalization of AMP-deaminase isozymes in human skeletal muscle and cultured muscle cells: concentration of isoform M at the neuromuscular junction. J Histochem Cytochem 42:861-868

Fig.1

Immunofluorescence microscopy: representative images of human skeletal muscle sections treated with anti-HRG and anti-myosin antibodies. Individual fluorescent channels: green (HRG) and red (myosin). (**a**) Cross sections incubated with HRG-462 or HRG-256 antibody. (**b**) Double immunofluorescence with HRG-462 and My-32 antibodies, performed on cross sections. I, type I muscle fiber; II, type II muscle fiber. (**c**) Double immunofluorescence with HRG-462 and My-32 antibodies, performed on longitudinal sections. Scale bars 100 µm for **a**, 50 µm for **b**, 10 µm for **c**

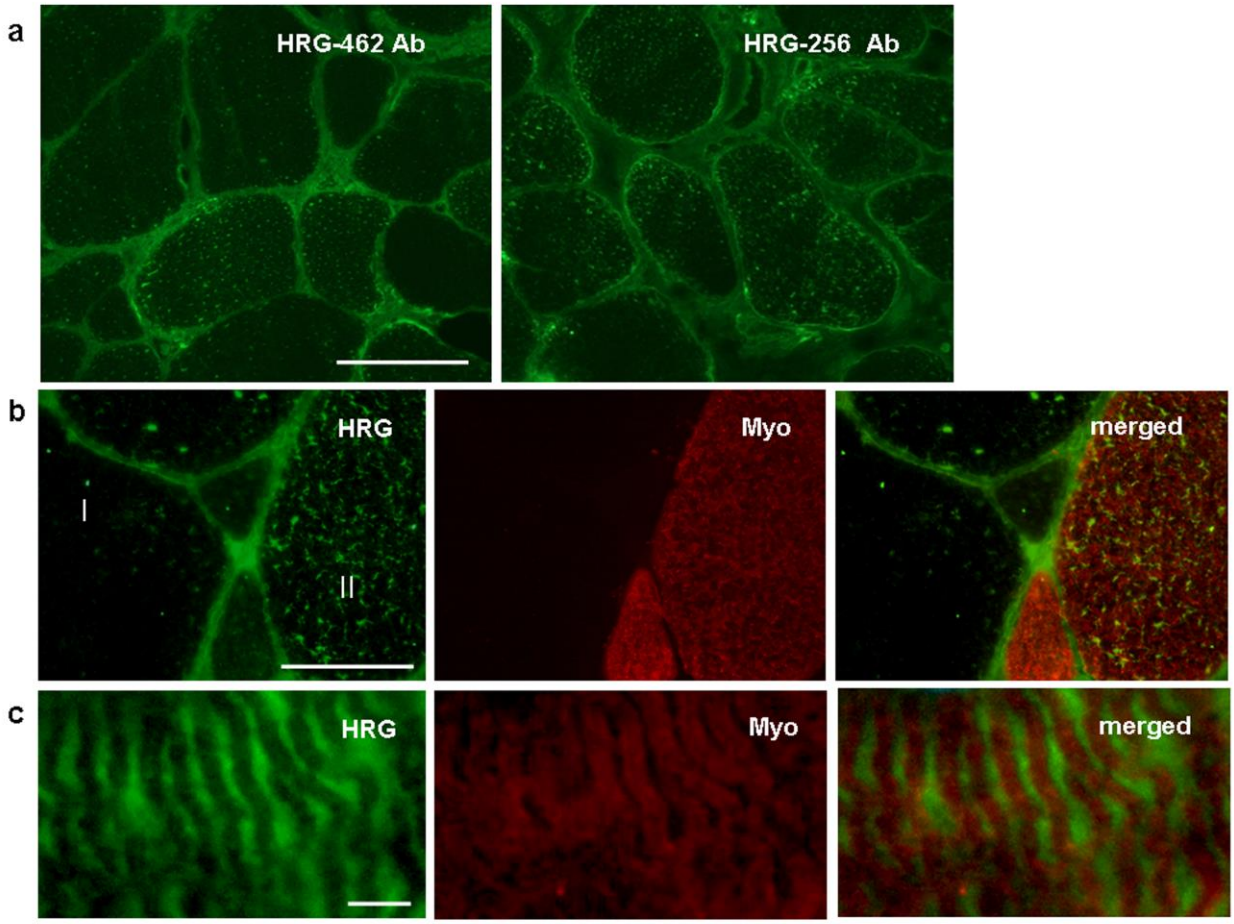

Fig.2

Confocal laser scanning microscopy: representative images of human skeletal muscle sections treated with HRG-462, anti-myosin and anti-actin antibodies. Individual fluorescent channels: red (HRG), green (myosin and actin) and blue (nuclei). (**a**) Three-dimensional picture of the maximum intensity projection of the raw images of longitudinal sections; capital letters A and I indicate the A-band and the I-band, respectively. (**b**) Images acquired in one Z-plane. The arrows point out the contact of HRG with the ends of the A-bands. The distribution of HRG is similar to that of actin. (**c**) Three-dimensional picture of the maximum intensity projection of the raw images of a cross section. HRG and actin, although closely associated, do not co-label (see arrows) as it is also evidenced in (**d**) by the isosurface representation. (**e**) The bi-dimensional image of the maximum intensity projection allows to observe the HRG immunopositivity also in the nuclei (arrowheads) as evidenced by the color overlap of the blue (nuclei) and red (HRG) fluorescent channels. Scale bars 2.5 µm for **a** and **b**, 10 µm for **c** and **e**

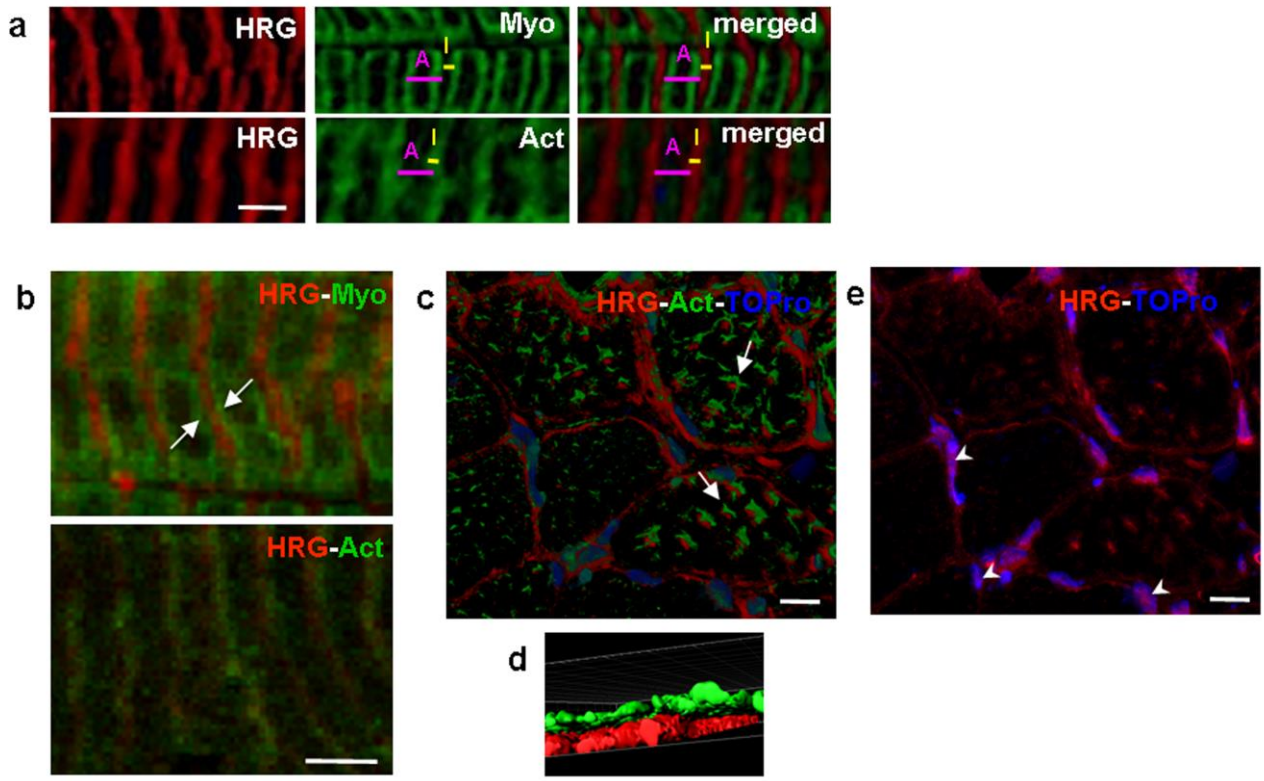

Fig.3

Confocal laser scanning microscopy: representative images of a human skeletal muscle myofibril treated with anti-AMPD1 (red) and My-32 (green) antibodies. In the longitudinal section, the AMPD1 staining is present all over the I-band (see arrows) as well as into the A-band (see arrowheads). Capital letters A and I indicate the A-band and the I-band, respectively. Scale bar 2.5 µm